

Magnetohydrodynamic Three-Dimensional Flow of a Second-Grade Fluid with Heat Transfer

Tasawar Hayat^{a,b} and Muhammad Nawaz^a

^a Department of Mathematics, Quaid-I-Azam University 45320, Islamabad 44000, Pakistan

^b Department of Mathematics, College of Sciences, KS University, P.O. Box 2455, Riyadh 11451, Saudi Arabia

Reprint requests to T. H.; E-mail: pensy_t@yahoo.com

Z. Naturforsch. **65a**, 683–691 (2010); received October 20, 2009

An analysis has been carried out for the heat transfer on steady boundary layer flow of a second-grade fluid bounded by a stretching sheet. The magnetohydrodynamic nature of the fluid is considered in the presence of Hall and ion-slip currents. The nonlinear mathematical problem is computed by a powerful tool, namely, the homotopy analysis method (HAM). A comparative study between the present and existing limiting results is carefully made. Convergence regarding the obtained solution is discussed. Skin friction coefficients and Nusselt number are analyzed. Effects of embedded parameters on the dimensionless velocities and temperature are examined.

Key words: Hall and Ion-Slip Currents; Stretching Surface; Skin Friction Coefficient; Nusselt Number.

1. Introduction

The boundary layer flow and the heat transfer in viscous and non-Newtonian fluids over a stretching sheet is important in industrial and engineering processes such as aerodynamic extrusion of plastic or rubber sheets, cooling of an infinite metallic plate in a cooling bath, extrusion of polymers or filament from a die, glass blowing, continuous casting, spinning of fibers, and crude oil extrusion. After the seminal study of Crane [1], several attempts [2–5] have been made on this topic. The heat transfer characteristics for such flows have been also studied by the researchers [6–16]. The quality and properties of the industrial products can be controlled by stretching rate, cooling rate, and magnetohydrodynamics (MHD). Besides this, the MHD flows are important in power generators, MHD accelerators, refrigerations coils, transmission lines, electric transformers, and heating elements. Some workers [17–19] have already reported the MHD flows in the presence of a Hall current. Such considerations of magnetohydrodynamic flow are useful in levitation and pumping of liquids in mechanical engineering, boundary layer control, and transpiration processes in aerodynamics.

However, the effect of heat transfer on three-dimensional stretching flow of a second-grade fluid with Hall and ion-slip currents has not been reported so far. Therefore, the main objective of this paper is to study such effects. In this paper we use the homo-

topy analysis method (HAM) [20–37] to solve the nonlinear system for heat transfer characteristics on the three-dimensional flow of a second-grade fluid. In Section 2, the mathematical formulation, definition of skin friction coefficients and Nusselt number are presented. Section 3 extends the application of HAM to construct series solutions of the governing nonlinear system. Section 4 analyzes the convergence of HAM solutions. In Section 5, the results and discussion are given. The results for limiting cases are compared with the already existing results [38–41]. The conclusions are summarized in Section 6.

2. Mathematical Formulation

We consider heat transfer characteristics on steady, laminar, and three-dimensional MHD flow of an incompressible second-grade fluid over a stretching surface coinciding the plane $y = 0$. The fluid is electrically conducting and the stretching surface is electrically non-conducting. A uniform magnetic field \mathbf{B}_0 is applied parallel to the y -axis. The effects of Hall and ion-slips currents are taken into account. Due to the Hall current, there is a force (Hall force) in z -direction which induces a cross flow in that direction and, hence, flow becomes three-dimensional. Furthermore, viscous dissipation and Joule heating are considered. The corresponding boundary layer equations are

$$\frac{\partial u}{\partial x} + \frac{\partial v}{\partial y} = 0, \quad (1)$$

$$u \frac{\partial u}{\partial x} + v \frac{\partial u}{\partial y} = v \frac{\partial^2 u}{\partial y^2} + \frac{\alpha_1}{\rho} \left[u \frac{\partial^3 u}{\partial x \partial y^2} + v \frac{\partial^3 u}{\partial y^3} \right. \\ \left. + \frac{\partial u}{\partial x} \frac{\partial^2 u}{\partial y^2} + \frac{\partial u}{\partial y} \frac{\partial^2 u}{\partial x \partial y} + \frac{\partial w}{\partial y} \frac{\partial^2 w}{\partial x \partial y} + \frac{\partial w}{\partial x} \frac{\partial^2 w}{\partial y^2} \right] \quad (2) \\ - \frac{\sigma B_0^2}{\rho[(1+p\beta_i)^2+p^2]} [(1+p\beta_i)u+pw],$$

$$u \frac{\partial w}{\partial x} + v \frac{\partial w}{\partial y} = v \frac{\partial^2 w}{\partial y^2} + \frac{\alpha_1}{\rho} \left[u \frac{\partial^3 w}{\partial x \partial y^2} + v \frac{\partial^3 w}{\partial y^3} \right] \quad (3) \\ + \frac{\sigma B_0^2}{\rho[(1+p\beta_i)^2+p^2]} [pu - (1+p\beta_i)w],$$

$$u \frac{\partial T}{\partial x} + v \frac{\partial T}{\partial y} = K \frac{\partial^2 T}{\partial y^2} + \frac{\sigma B_0^2}{\rho c_p [(1+p\beta_i)^2+p^2]} [u^2+w^2] \\ + \frac{v}{c_p} \left[\left(\frac{\partial u}{\partial y} \right)^2 + \left(\frac{\partial w}{\partial y} \right)^2 \right] + \frac{\alpha_1}{\rho c_p} \left[u \frac{\partial u}{\partial y} \frac{\partial^2 u}{\partial x \partial y} \right. \\ \left. + v \frac{\partial u}{\partial y} \frac{\partial^2 u}{\partial y^2} + v \frac{\partial w}{\partial y} \frac{\partial^2 w}{\partial y^2} + u \frac{\partial w}{\partial y} \frac{\partial^2 w}{\partial x \partial y} \right], \quad (4)$$

$$u = ax, \quad v = 0, \quad w = 0, \quad T = T_w, \quad \text{at } y = 0; \\ a > 0; \quad u \rightarrow 0, \quad w \rightarrow 0, \quad T \rightarrow T_\infty \quad \text{as } y \rightarrow \infty. \quad (5)$$

Here u , v , and w are the velocity components in x , y , and z -directions, $\alpha_1 (\geq 0)$ is the material constant, ν is the kinematics, ρ is the density of fluid, $\sigma (= e^2 n_e \tau_e / m_e)$ is the electrical conductivity, $p (= \omega_e \tau_e)$ is the Hall parameter, $\beta_i (= en_e B_0 / (1 + n_e / n_a) K_{ai})$ is the ion-slip parameter, τ_e is the electron collision time, m_e is the mass of the electron, ω_e is the electron frequency, n_e is the electron number density, n_a is the neutral particle density, K_{ai} is the friction coefficient between ions and neutral particles, K is the thermal conductivity, and c_p is the specific heat of the fluid.

Invoking similarity variables

$$u = axf'(\eta), \quad v = -\sqrt{av}f(\eta), \quad w = axg(\eta), \\ \theta(\eta) = \frac{T - T_\infty}{T_w - T_\infty}, \quad \eta = \sqrt{\frac{a}{\nu}}y, \quad (6)$$

in (1)–(5), one obtains

$$f''' - \frac{M}{(1+p\beta_i)^2+p^2} [(1+p\beta_i)f' + pg] + ff'' - (f')^2 \\ + \alpha[2f'f''' - ff^{(iv)} + (f'')^2 + (g')^2 + gg''] = 0, \quad (7) \\ g'' + \frac{M}{(1+p\beta_i)^2+p^2} [pf' - (1+p\beta_i)g] \\ - f'g + fg' + \alpha[f'g'' - fg'''] = 0,$$

$$\theta'' + Prf\theta' + \frac{PrEcM}{(1+p\beta_i)^2+p^2} [(f')^2 + g^2] \\ + PrEc[(f'')^2 + (g')^2] + \alpha PrEc[f'(g')^2 - fg'g'' \\ - ff''f''' + f'(f'')^2] = 0, \quad (8)$$

$$f(0) = 0, \quad f'(0) = 1, \quad f'(\infty) = 0, \quad g(0) = 0, \\ g(\infty) = 0, \quad \theta(0) = 1, \quad \theta(\infty) = 0, \quad (9)$$

in which

$$\alpha = \frac{\alpha_1 a}{\mu}, \quad M = \frac{\sigma B_0^2}{\rho a}, \quad Pr = \frac{\mu c_p}{K}, \quad Ec = \frac{(ax)^2}{c_p(T_w - T_\infty)},$$

respectively, are called the second-grade parameter, the Hartman number, the Prandtl number, and the local Eckert number. Here it is worth mentioning that the case for $p = 0$ corresponds to the situation when Hall current is absent and $\beta_i = 0$ corresponds to the case when ion-slip current is not present. The skin friction coefficients C_{f_x} , C_{g_x} and Nusselt number Nu_x are defined by the following expressions

$$C_{f_x} = \frac{\tau_{xy}|_{y=0}}{\rho(ax)^2} = \frac{1}{\rho(ax)^2} \left\{ \mu \frac{\partial u}{\partial y} \Big|_{y=0} + \alpha_1 \left[u \frac{\partial^2 u}{\partial x \partial y} \right. \right. \\ \left. \left. + v \frac{\partial^2 u}{\partial y^2} + 2 \frac{\partial u}{\partial x} \frac{\partial u}{\partial y} + \frac{\partial w}{\partial x} \frac{\partial w}{\partial y} \right] \Big|_{y=0} \right\} \quad (10) \\ = \frac{1+3\alpha}{\sqrt{Re_x}} f''(0),$$

$$C_{g_x} = \frac{\tau_{zy}|_{y=0}}{\rho(ax)^2} = \frac{1}{\rho(ax)^2} \left\{ \mu \frac{\partial w}{\partial y} \Big|_{y=0} + \alpha_1 \left[\frac{\partial u}{\partial x} \frac{\partial w}{\partial y} \right. \right. \\ \left. \left. + v \frac{\partial^2 w}{\partial y^2} - \frac{\partial w}{\partial x} \frac{\partial v}{\partial x} + u \frac{\partial^2 w}{\partial x \partial y} \right] \Big|_{y=0} \right\} \quad (11) \\ = \frac{1+3\alpha}{\sqrt{Re_x}} g'(0),$$

$$Nu_x = \frac{xh_w}{K} = - \frac{xK \frac{\partial T}{\partial y} \Big|_{y=0}}{K(T_w - T_\infty)} = -\sqrt{Re_x} \theta'(0), \quad (12)$$

where $Re_x = ax^2/\nu$ is called the local Reynolds number.

3. Solutions by Homotopy Analysis Method

3.1. Zeroth-Order Solutions

The HAM solutions $f(\eta)$, $g(\eta)$, and $\theta(\eta)$ in the form of base functions

$$\{\eta^k \exp(-n\eta), \quad k \geq 0, \quad n \geq 0\}, \quad (13)$$

can be expressed by the following infinite series:

$$\begin{aligned}
 f(\eta) &= a_{0,0}^0 + \sum_{n=1}^m \sum_{k=1}^m a_{m,n}^k \eta^k \exp(-n\eta), \\
 g(\eta) &= \sum_{n=1}^m \sum_{k=1}^m b_{m,n}^k \eta^k \exp(-n\eta), \\
 \theta(\eta) &= \sum_{n=1}^m \sum_{k=1}^m c_{m,n}^k \eta^k \exp(-n\eta),
 \end{aligned}
 \tag{14}$$

where $a_{m,n}^k$, $b_{m,n}^k$, and $c_{m,n}^k$ are the coefficients. Invoking the so-called rule of solution expressions, the initial guesses and linear operators \mathcal{L}_i ($i = 1-3$) are chosen as

$$\begin{aligned}
 f_0(\eta) &= 1 - \exp(-\eta), \quad g_0(\eta) = 0, \\
 \theta_0(\eta) &= \eta \exp(-\eta) + \exp(-\eta),
 \end{aligned}
 \tag{15}$$

$$\mathcal{L}_1[f(\eta)] = \frac{d^3 f}{d\eta^3} - \frac{df}{d\eta},$$

$$\mathcal{L}_2[g(\eta)] = \frac{d^2 g}{d\eta^2} - g,
 \tag{16}$$

$$\mathcal{L}_3[\theta(\eta)] = \frac{d^2 \theta}{d\eta^2} - \theta,$$

and the linear operators \mathcal{L}_i ($i = 1-3$) satisfy the following properties:

$$\begin{aligned}
 \mathcal{L}_1[C_1 + C_2 \exp(\eta) + C_3 \exp(-\eta)] &= 0, \\
 \mathcal{L}_2[C_4 \exp(\eta) + C_5 \exp(-\eta)] &= 0, \\
 \mathcal{L}_3[C_6 \exp(\eta) + C_7 \exp(-\eta)] &= 0,
 \end{aligned}
 \tag{17}$$

where C_i ($i = 1-7$) are arbitrary constants.

3.2. Zeroth-Order Formation Problems

The zeroth-order deformation problems are

$$\begin{aligned}
 (1-q)\mathcal{L}_1[\Phi(\eta;q) - f_0(\eta)] &= q\hbar_1 \mathcal{N}_1[\Phi(\eta;q), \Psi(\eta;q)], \\
 (1-q)\mathcal{L}_2[\Psi(\eta;q) - g_0(\eta)] &= q\hbar_2 \mathcal{N}_2[\Phi(\eta;q), \Psi(\eta;q)], \\
 (1-q)\mathcal{L}_3[\Theta(\eta;q) - \theta_0(\eta)] &= q\hbar_3 \mathcal{N}_3[\Phi(\eta;q), \Psi(\eta;q), \Theta(\eta;q)], \\
 \Phi(0;q) = 0, \quad \left. \frac{\partial \Phi(\eta;q)}{\partial \eta} \right|_{\eta=0} &= 1, \\
 \left. \frac{\partial \Phi(\eta;q)}{\partial \eta} \right|_{\eta \rightarrow \infty} = 0, \quad \Psi(0;q) = 0, \\
 \left. \frac{\partial \Psi(\eta;q)}{\partial \eta} \right|_{\eta \rightarrow \infty} = 0, \quad \Theta(0) = 1, \quad \Theta(\infty) = 0.
 \end{aligned}
 \tag{19}$$

In the above expressions $q \in [0, 1]$ and $\hbar_i \neq 0$ ($i = 1-3$) are the embedding and auxiliary parameters, respectively, and $\Phi(\eta;0) = f_0(\eta)$, $\Psi(\eta;0) = g_0(\eta)$, $\Theta(\eta;0) = \theta_0(\eta)$ and $\Phi(\eta;1) = f(\eta)$, $\Psi(\eta;1) = g(\eta)$, $\Theta(\eta;1) = \theta(\eta)$. When q varies from 0 to 1, then $\Phi(\eta;q)$ varies from the initial guess $f_0(\eta)$ to $f(\eta)$, $\Psi(\eta;q)$ varies from the initial guess $g_0(\eta)$ to $g(\eta)$, and $\Theta(\eta;q)$ varies from the initial guess $\theta_0(\eta)$ to $\theta(\eta)$. The nonlinear operators \mathcal{N}_i ($i = 1-3$) are given below:

$$\begin{aligned}
 \mathcal{N}_1[\Phi(\eta;q), \Psi(\eta;q)] &= \frac{\partial^3 \Phi(\eta;q)}{\partial \eta^3} - \frac{M}{(1+p\beta_1)^2 + p^2} \\
 &\cdot \left[(1+p\beta_1) \frac{\partial \Phi(\eta;q)}{\partial \eta} + p\Psi(\eta;q) \right] + \alpha \left[2 \frac{\partial \Phi(\eta;q)}{\partial \eta} \right. \\
 &\cdot \left. \frac{\partial^3 \Phi(\eta;q)}{\partial \eta^3} - \Phi(\eta;q) \frac{\partial^4 \Phi(\eta;q)}{\partial \eta^4} + \left(\frac{\partial^2 \Phi(\eta;q)}{\partial \eta^2} \right)^2 \right] \\
 &+ \alpha \left[\Psi(\eta;q) \frac{\partial^2 \Psi(\eta;q)}{\partial \eta^2} + \left(\frac{\partial \Psi(\eta;q)}{\partial \eta} \right)^2 \right] \\
 &+ \Phi(\eta;q) \frac{\partial^2 \Phi(\eta;q)}{\partial \eta^2} - \left(\frac{\partial \Phi(\eta;q)}{\partial \eta} \right)^2,
 \end{aligned}
 \tag{20}$$

$$\begin{aligned}
 \mathcal{N}_2[\Psi(\eta;q), \Phi(\eta;q)] &= \frac{\partial^2 \Psi}{\partial \eta^2} + \frac{M}{(1+p\beta_1)^2 + p^2} \\
 &\cdot \left[p \frac{\partial \Phi(\eta;q)}{\partial \eta} - (1+p\beta_1)\Psi(\eta;q) \right] \\
 &+ \alpha \left[\frac{\partial \Phi(\eta;q)}{\partial \eta} \frac{\partial^2 \Psi(\eta;q)}{\partial \eta^2} - \Phi(\eta;q) \frac{\partial^3 \Psi(\eta;q)}{\partial \eta^3} \right] \\
 &+ \Phi(\eta;q) \frac{\partial \Psi(\eta;q)}{\partial \eta} - \Psi(\eta;q) \frac{\partial \Phi(\eta;q)}{\partial \eta},
 \end{aligned}
 \tag{21}$$

$$\begin{aligned}
 \mathcal{N}_3[\Theta(\eta;q), \Psi(\eta;q), \Phi(\eta;q)] &= \frac{\partial^2 \Theta(\eta;q)}{\partial \eta^2} \\
 &+ Pr\Phi(\eta;q) \frac{\partial \Theta(\eta;q)}{\partial \eta} + \frac{PrEcM}{(1+p\beta_1)^2 + p^2} \\
 &\cdot \left[\left(\frac{\partial \Phi(\eta;q)}{\partial \eta} \right)^2 + (\Psi(\eta;q))^2 \right] + PrEc \left[\left(\frac{\partial^2 \Phi(\eta;q)}{\partial \eta^2} \right)^2 \right. \\
 &+ \left. \left(\frac{\partial \Psi(\eta;q)}{\partial \eta} \right)^2 \right] + \alpha PrEc \frac{\partial \Phi(\eta;q)}{\partial \eta} \left(\frac{\partial^2 \Phi(\eta;q)}{\partial \eta^2} \right)^2 \\
 &+ \alpha PrEc \frac{\partial \Phi(\eta;q)}{\partial \eta} \left(\frac{\partial \Psi(\eta;q)}{\partial \eta} \right)^2 \\
 &- \alpha PrEc \Phi(\eta;q) \frac{\partial \Psi(\eta;q)}{\partial \eta} \frac{\partial^2 \Psi(\eta;q)}{\partial \eta^2} \\
 &- \alpha PrEc \Phi(\eta;q) \frac{\partial^2 \Phi(\eta;q)}{\partial \eta^2} \frac{\partial^3 \Phi(\eta;q)}{\partial \eta^3}.
 \end{aligned}
 \tag{22}$$

By using Taylor’s theorem, one can write

$$\begin{aligned} \Phi(\eta; q) &= f_0(\eta, \xi) + \sum_{m=1}^{\infty} f_m(\eta, \xi) q^m, \\ \Psi(\eta; q) &= g_0(\eta) + \sum_{m=1}^{\infty} g_m(\eta) q^m, \\ \Theta(\eta; q) &= \theta_0(\eta) + \sum_{m=1}^{\infty} \theta_m(\eta) q^m, \end{aligned} \tag{23}$$

in which

$$\begin{aligned} f_m(\eta) &= \frac{1}{m!} \left. \frac{\partial^m \Phi(\eta; q)}{\partial q^m} \right|_{q=0}, \\ g_m(\eta) &= \frac{1}{m!} \left. \frac{\partial^m \Psi(\eta; q)}{\partial q^m} \right|_{q=0}, \\ \theta_m(\eta) &= \frac{1}{m!} \left. \frac{\partial^m \Theta(\eta; q)}{\partial q^m} \right|_{q=0}. \end{aligned} \tag{24}$$

3.3. Higher-Order Deformation Problems

Writing

$$\begin{aligned} f_m(\eta) &= \{f_0(\eta), f_1(\eta), f_2(\eta), f_3(\eta) \dots f_m(\eta)\}, \\ g_m(\eta) &= \{g_0(\eta), g_1(\eta), g_2(\eta), g_3(\eta) \dots g_m(\eta)\}, \\ \theta_m(\eta) &= \{\theta_0(\eta), \theta_1(\eta), \theta_2(\eta), \theta_3(\eta) \dots \theta_m(\eta)\}, \end{aligned} \tag{25}$$

the deformation problems at the m th-order are

$$\begin{aligned} \mathcal{L}_1[f_m(\eta) - \chi_m f_{m-1}(\eta)] &= \hbar_1 \mathcal{R}_{1m}(f_{m-1}(\eta)), \\ f_m(0) = 0, \quad f'_m(0) = 0, \quad f'_m(\infty) = 0, \\ \mathcal{L}_2[g_m(\eta) - \chi_m g_{m-1}(\eta)] &= \hbar_2 \mathcal{R}_{2m}(g_{m-1}(\eta)), \\ g_m(0) = 0, \quad g_m(\infty) = 0, \\ \mathcal{L}_3[\theta_m(\eta) - \chi_m \theta_{m-1}(\eta)] &= \hbar_3 \mathcal{R}_{3m}(\theta_{m-1}(\eta)), \\ \theta_m(0) = 1, \quad \theta_m(\infty) = 0, \\ \chi_m &= \begin{cases} 0, & m \leq 1, \\ 1, & m > 1, \end{cases} \end{aligned} \tag{26}$$

$$\begin{aligned} \mathcal{R}_{1m}(f_{m-1}(\eta), g_{m-1}(\eta)) &= f'''_{m-1}(\eta) \\ &- \frac{M}{(1+p\beta_i)^2+p^2} [(1+p\beta_i)f'_{m-1}(\eta) + pg_{m-1}(\eta)] \\ &+ \sum_{n=0}^{m-1} [f_n(\eta)f''_{m-1-n}(\eta) - f'_n(\eta)f'_{m-1-n}(\eta)] \\ &+ \alpha \sum_{n=0}^{m-1} [f''_n(\eta)f'_{m-1-n}(\eta) + 2f'_n(\eta)f'''_{m-1-n}(\eta) \\ &- f_n(\eta)f''''_{m-1-n}(\eta)] \end{aligned}$$

$$+ \alpha \sum_{n=0}^{m-1} [g_n(\eta)g''_{m-1-n}(\eta) + g'_n(\eta)g'_{m-1-n}(\eta)], \tag{27}$$

$$\begin{aligned} \mathcal{R}_{2m}(g_{m-1}(\eta), f_{m-1}(\eta)) &= g''_{m-1}(\eta) \\ &+ \frac{M}{(1+p\beta_i)^2+p^2} [pf'_{m-1}(\eta) - (1+p\beta_i)g_{m-1}(\eta)] \\ &+ \alpha \sum_{n=0}^{m-1} [f'_n(\eta)g''_{m-1-n}(\eta) - f_n(\eta)g'''_{m-1-n}(\eta)] \end{aligned} \tag{28}$$

$$+ \sum_{n=0}^{m-1} [f_n(\eta)g'_{m-1-n}(\eta) - f'_n(\eta)g_{m-1-n}(\eta)],$$

$$\begin{aligned} \mathcal{R}_{3m}(\theta_{m-1}(\eta), f_{m-1}(\eta), g_{m-1}(\eta)) &= \theta''_{m-1}(\eta) \\ &+ Pr \sum_{n=0}^{m-1} f_n(\eta)\theta'_{m-1-n}(\eta) + \frac{PrEcM}{(1+p\beta_i)^2+p^2} \\ &\cdot \sum_{n=0}^{m-1} [f'_n(\eta)f'_{m-1-n}(\eta) + g_n(\eta)g_{m-1-n}(\eta)] \end{aligned}$$

$$+ PrEc \sum_{n=0}^{m-1} [f''_n(\eta)f'_{m-1-n}(\eta) + g'_n(\eta)g'_{m-1-n}(\eta)]$$

$$- \alpha PrEc \sum_{l=0}^n \sum_{n=0}^{m-1} f_{m-1-n}(\eta)f''_{n-l}(\eta)f'''_l(\eta)$$

$$+ \alpha PrEc \sum_{l=0}^n \sum_{n=0}^{m-1} f'_{m-1-n}(\eta)f''_{n-l}(\eta)f'_l(\eta)$$

$$+ \alpha PrEc \sum_{l=0}^n \sum_{n=0}^{m-1} f'_{m-1-n}(\eta)g'_{n-l}(\eta)g'_l(\eta)$$

$$- \alpha PrEc \sum_{l=0}^n \sum_{n=0}^{m-1} f_{m-1-n}(\eta)g'_{n-l}(\eta)g''_l(\eta).$$

The general solutions of problems (27) are

$$\begin{aligned} f(\eta) &= f^*(\eta) + C_1^m + C_2^m \exp(\eta) + C_3^m \exp(-\eta), \\ g(\eta) &= g^*(\eta) + C_4^m \exp(\eta) + C_5^m \exp(-\eta), \\ \theta(\eta) &= \theta^*(\eta) + C_6^m \exp(\eta) + C_7^m \exp(-\eta), \end{aligned} \tag{30}$$

where $f^*(\eta)$ and $g^*(\eta)$ are particular solutions of problems (27).

4. Convergence of HAM Solutions

The convergence of the HAM solutions and their rate of approximations strongly depend upon the values of the auxiliary parameters. For this purpose \hbar_i -curves are plotted through Figures 1–3. These figures clearly indicate that the admissible ranges for \hbar_i are $-0.95 \leq \hbar_1 \leq -0.45$, $-1 \leq \hbar_2 \leq -0.45$, and $-1.3 \leq \hbar_3 \leq -0.45$. In order to ensure the convergence of the

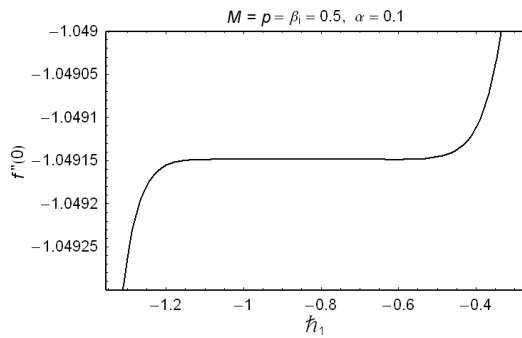


Fig. 1. \tilde{h}_1 -curve for $f''(0)$.

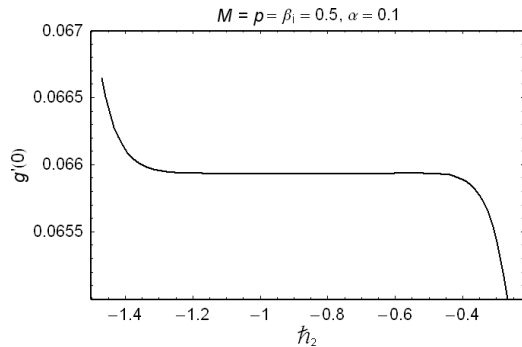


Fig. 2. \tilde{h}_2 -curve for $g'(0)$.

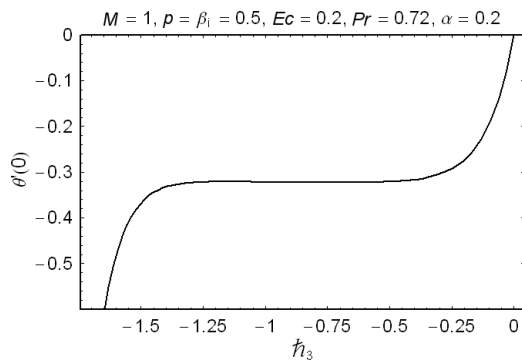


Fig. 3. \tilde{h}_3 -curve for $\theta'(0)$.

solutions, Table 1 is constructed. This table shows that the convergence is achieved at 40th-order of approximations.

5. Results and Discussion

The purpose of this section is to see the influence of the pertinent parameters on the dimensionless tangential velocity $f'(\eta)$, lateral velocity $g(\eta)$, and dimensionless temperature $\theta(\eta)$. Figures 4–7 describe the effects of Hartman number M , second-grade pa-

Table 1. Convergence of HAM solutions for different order of approximations when $M = 1, p = \beta_i = Ec = 0.5, \alpha = 0.1, Pr = 0.72, \tilde{h}_1 = \tilde{h}_3 = \tilde{h}_3 = -0.8$.

Order of approximations	$-f''(0)$	$g'(0)$	$\theta'(0)$
1	1.182528736	0.1103448276	0.121434
5	1.178409858	0.1130652923	0.146520
10	1.178434974	0.1130721256	0.141908
15	1.178434970	0.1130721355	0.138153
20	1.178434970	0.1130721354	0.13615
25	1.178434970	0.1130721354	0.13450
30	1.178434970	0.1130721354	0.13451
35	1.178434970	0.1130721354	0.13412
40	1.178434970	0.1130721354	0.13401
42	1.178434970	0.1130721354	0.13401
44	1.178434970	0.1130721354	0.13401

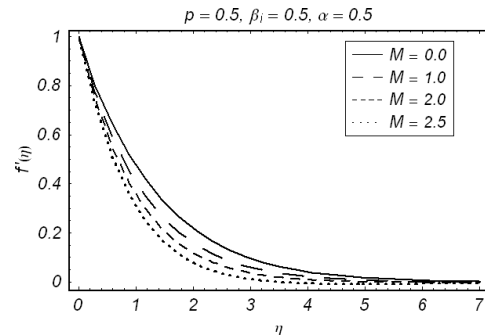


Fig. 4. Influence of M on $f'(\eta)$.

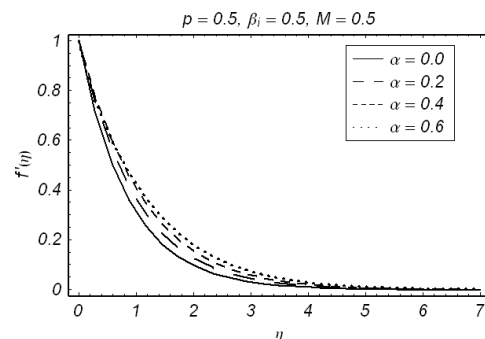


Fig. 5. Influence of α on $f'(\eta)$.

rameter α , Hall parameter p , and ion-slip parameter β_i on the dimensionless tangential velocity $f'(\eta)$. Figures 8–11 show the variation of the dimensionless lateral velocity $g(\eta)$ for various values of M, α, β_i , and p and Figures 12–17 represent the influence of M, β_i, p, Pr , and Ec on the dimensionless temperature. Figure 4 shows that the dimensionless tangential velocity $f'(\eta)$ decreases with an increase of the Hartman number M . This figure also indicates that the boundary layer thickness decreases when M is increased. From Figure 5 one can see that $f'(\eta)$ increases when

Table 2. Comparison of the values of $\theta'(0)$ for various of Pr when $M = \beta_i = p = Ec = \alpha = 0$.

Pr	Gupta and Gupta [38]	Grubka and Bobba [39]	Ali [40]	Salem [41]	Present results
0.7			-0.45255	-0.45605	-0.45394
1.0	-0.5820	-0.5820	-0.59988	-0.58223	-0.58197
10.0		-2.3080	2.29589	-2.30789	-2.30806

Table 3. Variation of skin friction coefficients for various values of M , α , p , and β_i when $h_i = -0.9$.

M	α	p	β_i	$-(Re_x)^{1/2}C_{f_x}$	$(Re_x)^{1/2}C_{g_x}$
0.0	0.1	0.5	0.1	1.17479	0.000000
0.5				1.38741	0.112205
1.0				1.57482	0.190247
1.5				1.74309	0.252128
1.0	0.0	0.5	0.5	1.30575	0.118612
	0.1			1.53197	0.146994
	0.2			1.73331	0.172694
	0.3			1.91639	0.196193
1.0	0.1	0.0	0.5	1.65837	0.000000
		0.5		1.63573	0.0441140
		1.0		1.61020	0.0800857
		1.5		1.58361	0.1085410
1.0	0.1	0.5	0.0	1.58674	0.203916
			0.2	1.56338	0.177857
			0.4	1.54197	0.156350
			0.6	1.52240	0.138434

Table 4. Variation of Nusselt number Nu_x for various values of M , α , p , β_i , Pr , and Ec when $h_i = -0.9$.

M	α	p	β_i	Pr	Ec	$-(Re_x)^{-1/2}Nu_x$
0.0	0.1	0.5	0.5	0.72	0.5	0.322583
0.5						0.221351
1.0						0.135440
1.5						0.061121
1.0	0.0	0.5	0.5	0.72	0.5	0.126223
	0.1					0.136803
	0.2					0.144720
	0.3					0.150787
1.0	0.1	0.0	0.5			0.322583
		0.5				0.221351
		1.0				0.135440
		1.5				0.061121
1.0	0.1	0.5	0.0	0.72	0.5	0.096266
			0.5			0.142932
			1.0			0.174617
			1.5			0.196692
1.0	0.1	0.5	0.5	0.02	0.5	0.122447
				0.37		0.115851
				0.72		0.135440
				1.07		0.151798
1.0	0.1	0.5	0.5	0.72	0.0	-0.422768
					0.5	-0.134301
					1.0	0.154166
					1.5	0.442633

the second grade parameter α increases and consequently the boundary layer thickness increases. The

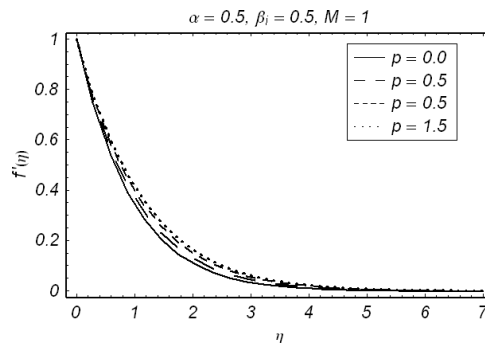


Fig. 6. Influence of p on $f'(\eta)$.

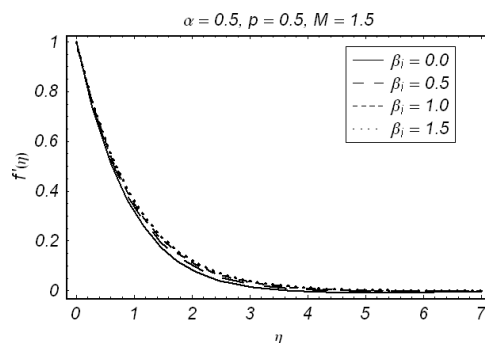


Fig. 7. Influence of β_i on $f'(\eta)$.

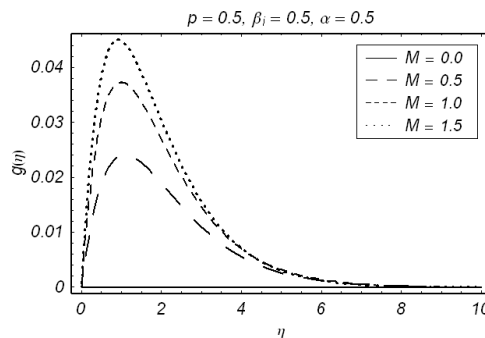


Fig. 8. Influence of M on $g(\eta)$.

dimensionless tangential velocity $f'(\eta)$ is an increasing function of Hall and ion-slip parameters (Figs. 6 and 7). From these figures one can see that the boundary layer thickness increases by increasing β_i and p . Figure 8 elucidates that the lateral velocity $g(\eta)$ increases with an increase of Hartman number M . This

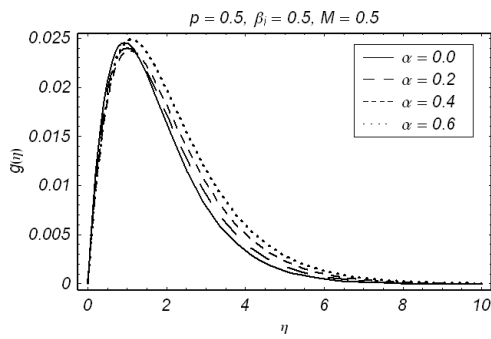


Fig. 9. Influence of α on $g(\eta)$.

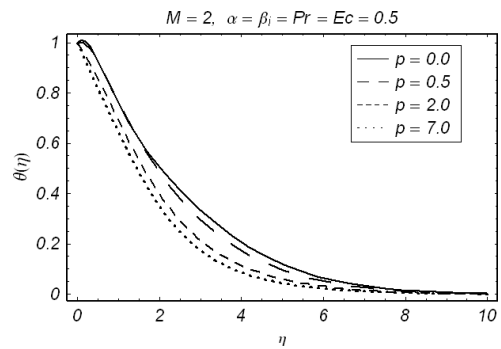


Fig. 13. Influence of p on $\theta(\eta)$.

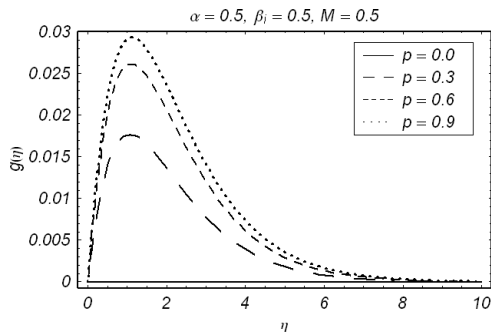


Fig. 10. Influence of p on $g(\eta)$.

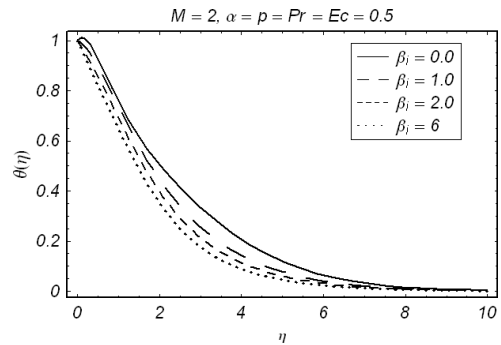


Fig. 14. Influence of β_i on $\theta(\eta)$.

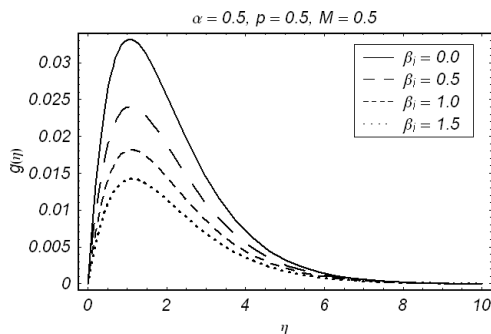


Fig. 11. Influence of β_i on $g(\eta)$.

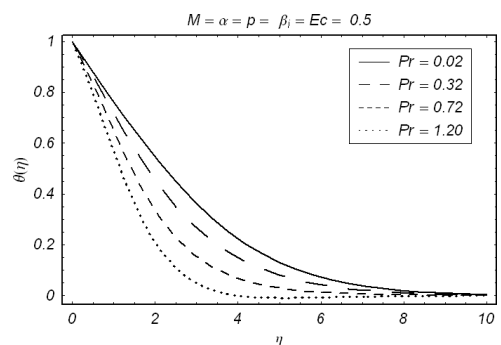


Fig. 15. Influence of Pr on $\theta(\eta)$.

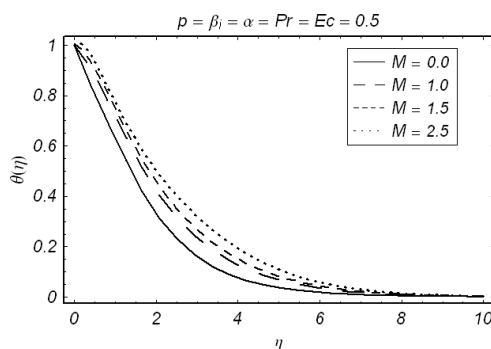


Fig. 12. Influence of M on $\theta(\eta)$.

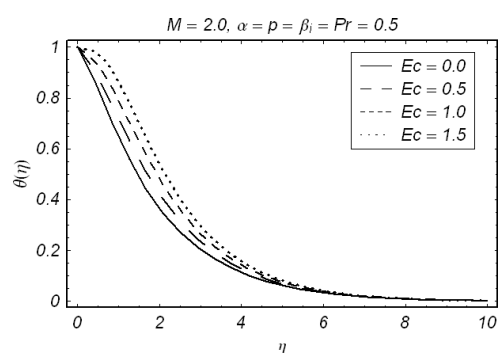


Fig. 16. Influence of Ec on $\theta(\eta)$.

figure also shows that the dimensionless lateral velocity $g(\eta) = 0$ for $M = 0$ ($p = 0$) which is expected since the flow in z -direction is due to the Hall effect. Figure 9 depicts that $g(\eta)$ decreases near the stretching sheet by increasing the second-grade parameter α but increases away from the stretching sheet. Figure 10 represents that the dimensionless lateral velocity $g(\eta)$ increases when the Hall parameter p is increased. Furthermore, one can see that for $p = 0$ (in the absence of Hall current) $g(\eta) = 0$ and the flow becomes two dimensional. Lateral velocity $g(\eta)$ is a decreasing function of the ion-slip parameter β_i (Fig. 11). Figures 8–11 elucidate that the boundary layer thickness corresponding to the lateral velocity $g(\eta)$ increases when M , α , and p are increased but it decreases with an increase in β_i . Figures 12 and 16 indicate the increasing trend of the dimensionless temperature $\theta(\eta)$ when M and Ec are increased, whereas it decreases by increasing p , β_i , and Pr (Figs. 13–15). From Figures 12–16 one can see that the thermal boundary layer increases by increasing M and Ec but it is a decreasing function of p , β_i , and Pr . Table 2 is constructed to analyze the influence of the parameters on the skin friction coefficients C_{fx} and C_{gz} in x and z -directions, respectively. From this table one can depict that the skin friction coefficients C_{fx} and C_{gz} increase when M and α are increased but decrease with an increase of β_i . From this table one can also see that effect of p on $(Re_x)^{1/2}C_{fx}$ and $(Re_x)^{1/2}C_{gz}$ is opposite. Table 3 gives the comparison between the present and already existing results for the special case when $M = \beta_i = p = Ec = \alpha = 0$. This table shows an excellent agreement between the present and existing limiting results. Table 4 is constructed to analyze the effects of different parameters on the local Nusselt number $(Re_x)^{-1/2}Nu_x$. This table shows that the local Nusselt Number is an increasing function of α , β_i , and Pr whereas it decreases when M , p , and Ec are increased.

6. Final Remarks

In this paper, we have investigated the effect of heat transfer on magnetohydrodynamic (MHD) steady

flow of an incompressible second-grade fluid in the presence of Hall and ion-slip currents. Resulting problems are solved analytically by the homotopy analysis method (HAM). Main findings of the analysis can be summarized as follows:

- Dimensionless tangential velocity $f'(\eta)$ is a decreasing function of M whereas dimensionless lateral velocity $g(\eta)$ increases by increasing M .
- Effect of β_i on $f'(\eta)$ is opposite to that of β_i on $g(\eta)$ but p has the similar effects on $f'(\eta)$ and $g(\eta)$.
- Qualitatively, behaviour of α on $f'(\eta)$ and $g(\eta)$ is similar.
- Effects of p and β_i on $f'(\eta)$ are similar.
- Behaviour of M is opposite to that of p , β_i , and Pr on $\theta(\eta)$ but similar to that of Ec .
- Effects of p and β_i on $f'(\eta)$ and $\theta(\eta)$ are opposite.
- Qualitatively, influence of β_i on $g(\eta)$ and $\theta(\eta)$ is opposite.
- Skin friction coefficient $(Re_x)^{1/2}C_{fx}$ is an increasing function of M and α whereas it decreases when p and β_i are increased.
- $(Re_x)^{1/2}C_{gz}$ increases by increasing M , α , and p and decreases with an increase in β_i .
- Effects of Pr and Ec on $\theta(\eta)$ are opposite.
- $(Re_x)^{-1/2}Nu_x$ is an increasing function of α , β_i , Pr , and Ec but it decreases when p is increased.
- Boundary layer thickness corresponding to tangential velocity $f'(\eta)$ can be reduced by applying magnetic field, and Boundary layer thickness corresponding to lateral velocity $g(\eta)$ can be decreased by ion-slip current.
- Thermal boundary layer thickness can be controlled through p , β_i , and Pr .

Acknowledgement

Authors are thankful to the Higher Education Commission (HEC) of Pakistan for the financial support.

- [1] L. J. Crane, J. Appl. Math. Phys. (ZAMP) **21**, 645 (1970).
- [2] T. Hayat, Q. Hussain, and T. Javed, Nonlinear Anal.: Real World Appl. **10**, 966 (2009).
- [3] M. Ayub, H. Zaman, M. Sajid, and T. Hayat, Commun. Nonlinear Sci. Numer. Simul. **13**, 1822 (2008).
- [4] T. Hayat and T. Javed, Phys. Lett. A **370**, 243 (2007).
- [5] T. Hayat, Z. Abbas, and M. Sajid, Phys. Lett. A **358**, 396 (2006).
- [6] T. Hayat, M. Sajid, and I. Pop, Nonlinear Anal.: Real World Appl. **9**, 1811 (2008).

- [7] M. Sajid, T. Hayat, and S. Asghar, *Int. J. Heat Mass Transf.* **50**, 1723 (2007).
- [8] R. C. Bataller, *Int. J. Heat Mass Transf.* **50**, 3152 (2007).
- [9] Z. Abbas, Y. Wang, T. Hayat, and M. Oberlack, *Int. J. Nonlinear Mech.* **43**, 783 (2008).
- [10] K.V. Prasad and K. Vajravelu, *Int. J. Heat Mass Transf.* **52**, 4956 (2009).
- [11] I. C. Liu, *Int. J. Heat Mass Transf.* **47**, 4427 (2004).
- [12] K. V. Prasad, D. Pal, V. Umesh, and N. S. P. Rao, *Commun. Nonlinear Sci. Numer. Simul.* **15**, 331 (2010).
- [13] R. C. Bataller, *Comp. Math. Appl.* **53**, 305 (2007).
- [14] R. C. Bataller, *J. Mater. Proc. Tech.* **203**, 176 (2008).
- [15] T. Hayat, T. Javed, and Z. Abbas, *Int. J. Heat Mass Transf.* **5**, 4528 (2008).
- [16] T. Hayat, S. Saif, and Z. Abbas, *Phys. Lett. A* **372**, 5037 (2008).
- [17] E. M. Abo-Eldahab and M. E. Elbarbary, *Int. J. Eng. Sci.* **39**, 1641 (2001).
- [18] E. M. Abo-Eldahab and A. M. Saleem, *Int. Commun. Heat Mass Transf.* **31**, 343 (2004).
- [19] T. Hayat, Z. Abbas, and S. Asghar, *Commun. Nonlinear Sci. Numer. Simul.* **13**, 2177 (2008).
- [20] T. Hayat, M. Nawaz, M. Sajid, and S. Asghar, *Comp. Math. Appl.* **58**, 369 (2009).
- [21] S. J. Liao, *Beyond perturbation: Introduction to homotopy analysis method*, Chapman and Hall, CRC Press, Boca Raton 2003.
- [22] S. J. Liao, *Appl. Math. Comp.* **147**, 499 (2004).
- [23] S. J. Liao, *Int. J. Heat Mass Transf.* **48**, 2529 (2005).
- [24] J. Cheng, S. J. Liao, R. N. Mohapatra, and K. Vajravelu, *J. Math. Anal. Appl.* **343**, 233 (2008).
- [25] S. Abbasbandy and E. J. Parkes, *Chaos, Soliton, and Fractals* **36**, 581 (2008).
- [26] S. Abbasbandy, *Chem. Eng. J.* **136**, 144 (2008).
- [27] S. Abbasbandy and F. S. Zakaria, *Nonlinear Dyn.* **51**, 83 (2008).
- [28] I. Hashim, O. Abdulaziz, and S. Momani, *Commun. Nonlinear Sci. Numer. Simul.* **14**, 674 (2009).
- [29] A. S. Bataineh, M. S. M. Noorani, and I. Hashim, *Commun. Nonlinear Sci. Numer. Simul.* **14**, 409 (2009).
- [30] F. M. Allan, *Appl. Math. Comp.* **190**, 6 (2007).
- [31] M. Sajid and T. Hayat, *Int. Commun. Heat Mass Transf.* **36**, 59 (2009).
- [32] M. Sajid, M. Awais, S. Nadeem, and T. Hayat, *Comp. Math. Appl.* **56**, 2019 (2008).
- [33] T. Hayat, Z. Abbas, T. Javed, and M. Sajid, *Chaos, Solitons, and Fractals*, **39**, 1615 (2009).
- [34] M. Sajid, I. Ahmad, T. Hayat, and M. Ayub, *Commun. Nonlinear Sci. Numer. Simul.* **13**, 2193 (2008).
- [35] T. Hayat, M. Sajid, and M. Ayub, *Commun. Nonlinear Sci. Numer. Simul.* **12**, 1481 (2007).
- [36] T. Hayat, Z. Abbas, and M. Sajid, *Phys. Lett. A* **372**, 2400 (2008).
- [37] M. Sajid and T. Hayat, *Chaos, Solitons, and Fractals* **39**, 1317 (2009).
- [38] P. S. Gupta and T. S. Gupta, *Can. J. Chem. Eng.* **55**, 744 (1977).
- [39] L. J. Grukba and K. M. Bobba, *ASME J. Heat Transf.* **107**, 248 (1985).
- [40] M. E. Ali, *Int. J. Heat Fluid Flow* **16**, 280 (1995).
- [41] A. M. Salem and M. A. El-Aziz, *Appl. Math. Model.* **32**, 1236 (2008).